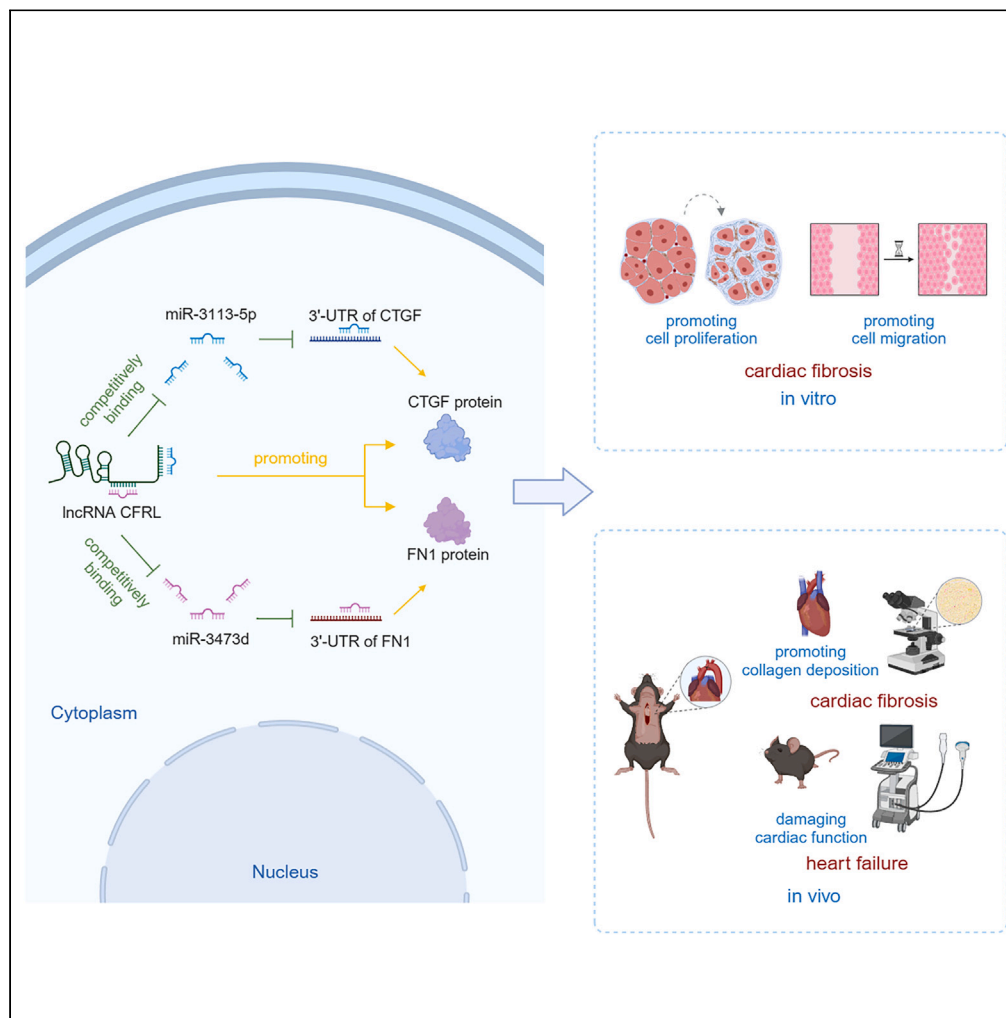


Article

LncRNA CFRL aggravates cardiac fibrosis by modulating both miR-3113-5p/CTGF and miR-3473d/FN1 axis



Yue Cui, Bozhong Shi, Zijie Zhou, ..., Zhongqun Zhu, Jinghao Zheng, Xiaomin He

zhengjh210@163.com (J.Z.)
mrxmhe@163.com (X.H.)

Highlights

CFRL is up-regulated in TAC-induced chronic pressure-overloaded heart failure mice

CFRL regulates cardiac fibrosis by sponging both miR-3113-5p and miR-3473d

CFRL targets two well-known fibrosis genes, CTGF and FN1, via ceRNA network

Silencing CFRL mitigates cardiac fibrosis and protects cardiac function in TAC mice



Article

LncRNA CFRL aggravates cardiac fibrosis by modulating both miR-3113-5p/CTGF and miR-3473d/FN1 axis

Yue Cui,^{1,2} Bozhong Shi,^{1,2} Zijie Zhou,^{1,2} Bo Chen,¹ Xiaoyang Zhang,¹ Cong Li,¹ Kai Luo,¹ Zhongqun Zhu,¹ Jinghao Zheng,^{1,*} and Xiaomin He^{1,3,*}

SUMMARY

Cardiac fibrosis is a major type of adverse remodeling, predisposing the disease progression to ultimate heart failure. However, the complexity of pathogenesis has hampered the development of therapies. One of the key mechanisms of cardiac diseases has recently been identified as long non-coding RNA (lncRNA) dysregulation. Through *in vitro* and *in vivo* studies, we identified an lncRNA NONMMUT067673.2, which is named as a cardiac fibrosis related lncRNA (CFRL). CFRL was significantly increased in both mouse model and cell model of cardiac fibrosis. *In vitro*, CFRL was proved to promote the proliferation and migration of cardiac fibroblasts by competitively binding miR-3113-5p and miR-3473d and indirectly up-regulating both CTGF and FN1. *In vivo*, silencing CFRL significantly mitigated cardiac fibrosis and improved left ventricular function. In short, CFRL may exert an essential role in cardiac fibrosis and interfering with CFRL might be considered as a multitarget strategy for cardiac fibrosis and heart failure.

INTRODUCTION

Cardiac fibrosis is a major type of adverse remodeling in response to chronic pressure overload. The aberrant proliferation of fibroblasts and excessive deposition of extracellular matrix (ECM) discoordinate myocardial excitation-contraction coupling, impair systolic and diastolic function, and thus predisposing the disease progression to ultimate heart failure (HF).^{1–3} However, the wide variety of molecular signals implicated in the fibrotic progress and the complexity of their interactions has hampered understanding the mechanistic basis of cardiac fibrosis.⁴ Therefore, there is few effective therapeutics for cardiac fibrosis in clinical practice, and further mechanistic studies are necessary for developing strategies and improving treatment efficacy.

In the development and progression of cardiac fibrosis, the deposition of ECM plays a vital role. The activated cardiac fibroblasts (CFs) undergo a series of transcriptome changes and produce non-cellular three-dimensional macromolecules to disrupt the myocardial architecture. Importantly, CFs upregulated two well-known fibrotic protein-coding genes, connective tissue growth factor (CTGF) and fibronectin 1 (FN1), to promote cell proliferation, motility, adhesion, and matrix turnover. The two culprit genes have become novel therapeutic targets to prevent cardiac fibrosis in recent endeavors. CTGF-neutralizing antibody pamrevlumab or FN1 inhibitor pUR4, respectively, attenuated fibrosis and presented protective effect in mouse HF model.^{5,6} However, limited studies attempt to combine the multitarget, where suppressing both genes necessitate drug regimens with unwarranted effect. Exploring a common upstream of CTGF and FN1 helps to develop a simplified therapeutic method to improve treatment efficacy.

To this end, long non-coding RNAs (lncRNAs) have become increasingly intriguing in regulating multitargets. They are transcripts of > 200 nucleotides in length without protein-coding function that arise from intergenic, antisense or promoter-proximal regions.⁷ Growing evidence has indicated that lncRNAs can function as competing endogenous RNA (ceRNA). In ceRNA network, lncRNAs sponge and block the effect of miRNAs, a class of ncRNA that suppresses target genes expression at their translational level.⁸ As one lncRNA can regulate multiple miRNAs, lncRNAs are able to form a complex regulatory network and regulate multitargets.⁹ The advent of deep sequencing led to the identification of a considerable amount of lncRNAs, which are increasingly recognized for their functions in controlling cardiovascular diseases.¹⁰

In the present study, we discovered a long non-coding RNA, lncRNA NONMMUT067673.2, in transverse aorta constriction (TAC) mice model to promote cardiac fibrosis by targeting both CTGF and FN1, named cardiac fibrosis related lncRNA (CFRL) in the following section.

¹Department of Cardiothoracic Surgery, Shanghai Children's Medical Center Affiliated to Shanghai Jiao Tong University School of Medicine, 1678 Dongfang Road, Shanghai 200127, China

²These authors contributed equally

³Lead contact

*Correspondence: zhengjh210@163.com (J.Z.), mrxmhe@163.com (X.H.)
<https://doi.org/10.1016/j.isci.2023.108039>



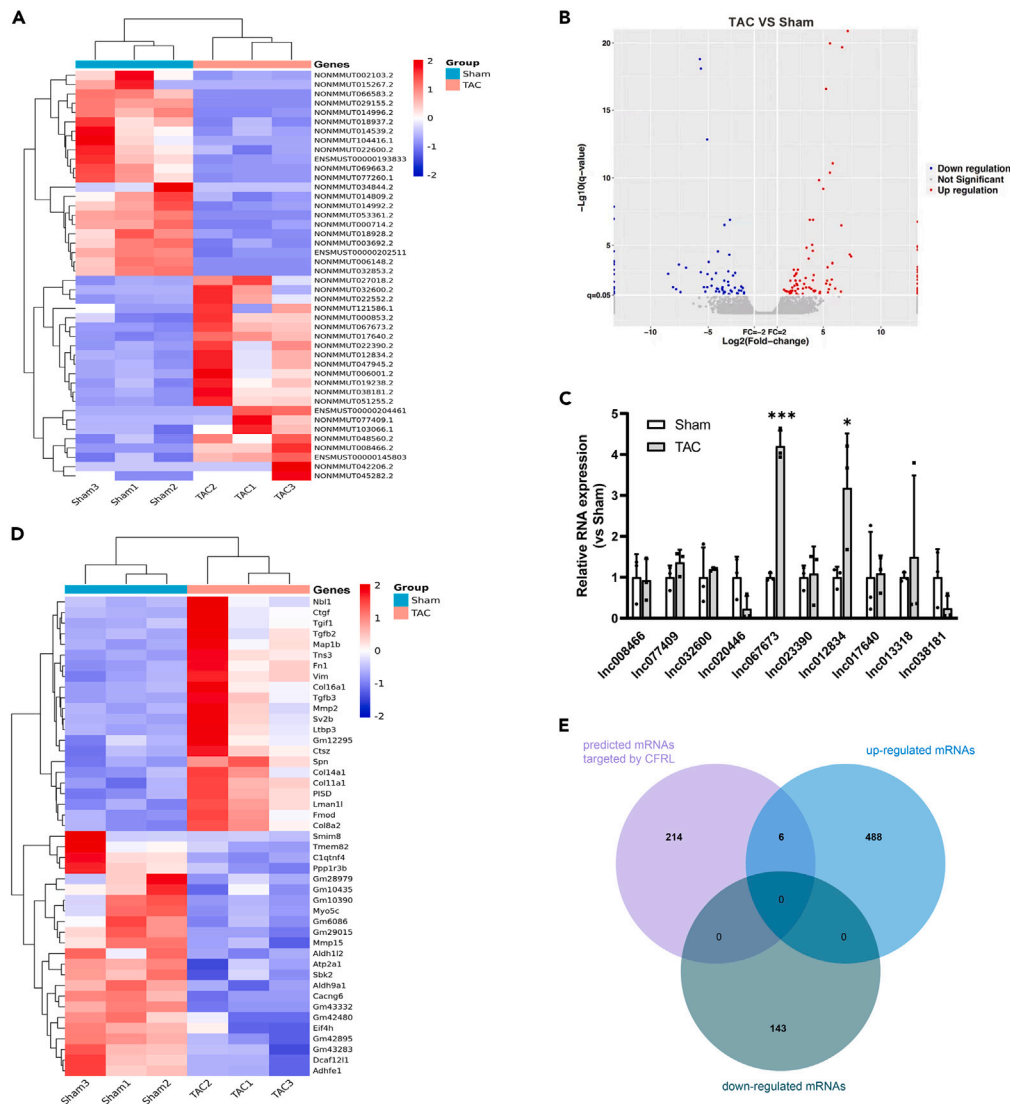


Figure 1. Increased expression of lncRNA NONMMUT067673.2 (CFRL) in LVs of TAC mice

(A) The results from hierarchical clustering showing the distinct lncRNA expression profiles between TAC and sham. “Red” indicated high relative expression and “blue” low relative expression.

(B) Volcano plot provided a convenient way to visualize the distribution of datasets of lncRNAs. Red plots represented up regulation and blue plots meant down regulation.

(C) qRT-PCR analysis showing dysregulated lncRNAs in LVs of TAC mice, including up-regulated CFRL. GAPDH mRNA served as an internal control. $n = 3$ mice. $**p < 0.01$ vs. Sham.

(D) The hierarchical clustering showing the distinct mRNA expression between TAC and sham.

(E) Venn diagram showing the intersection of the predicted mRNAs targeted by CFRL and the differential mRNAs.

RESULTS

Up-regulation of CFRL in TAC-induced mice

To study chronic pressure-overloaded HF, transverse aortic constriction mice model was established. After 6 weeks, a whole transcriptome RNA-sequencing was performed in left ventricle (LV) tissues isolated from mice undergoing TAC or sham surgery ($n = 3$ vs. 3). Differentially expressed RNAs were filtered by fold change ≥ 2.0 or ≤ 0.5 . We found 179 (97 up and 82 down) of 43234 detected lncRNAs that were significant different between TAC and sham LVs ($FDR < 0.05$) (Figures 1A, 1B, and Table S1).

Since it was easier to knockdown an lncRNA compared with overexpressing it, suppressing pro-fibrotic lncRNAs might be an effective treatment for cardiac fibrosis. We then performed qRT-PCR to detect the expression of top-ten upregulated lncRNAs found by RNA-seq.

Among them, lncRNA NONMMUT067673.2 (Figure S1), named CFRL in the following section, was markedly increased in the LV tissue of TAC-induced mice (Figure 1C). In brief, our findings suggested that CFRL was increased in mouse model of HF.

Target genes of lncRNA were predicted by *trans*-regulation and *cis*-regulation. And the Pearson correlation coefficient was used to test the expression correlation of lncRNAs and mRNAs. There were 637 (494 up and 143 down) of 20968 mRNAs significant different between TAC and sham LVs (FDR <0.05) (Figure 1D and Table S1). The intersection of the target genes and the differential mRNAs was taken subsequently (Figure 1E), including Anxa4, Slc13a4, FN1, Acta1, Gas2l3, and Ctgf. Among them, CTGF and FN1 were significantly up-regulated and had been proved to participate in fibrosis. We thus predicted that CTGF and FN1 might both be the target genes of CFRL.

CFRL increases cell viability and proliferation by targeting both CTGF and FN1 in mouse cardiac fibroblasts (mCFs)

Since CFRL might target two well-known fibrosis genes, it was speculated to participate in the pathologic process of cardiac fibrosis. To verify the hypothesis, we treated mouse cardiac fibroblasts (mCFs) with angiotensin II (Ang II, 100 nM), and discovered that the level of CFRL in mCFs was significantly raised (Figures 2A and S2B). However, AngII-treated mouse cardiomyocytes (mCMs) did not show the increase of CFRL, indicating a less important role of CFRL in cardiomyocytes (Figure S2A). Moreover, CFRL expression in AngII-treated mCFs was also higher than that in AngII-treated mCMs (Figure 2B). For further confirming the correlation of CFRL and CTGF/FN1, the plasmid DNA of CFRL was constructed and transfected into mCFs to overexpress CFRL (oe-CFRL). RT-qPCR results showed that CTGF and FN1 were both up-regulated after the overexpression of CFRL in mCFs (Figures S3A, 2C, and 2D). Meanwhile, the CTGF and FN1 protein levels examined by western Blot were elevated upon CFRL overexpression in mCFs (Figure 2E and S8A). To assess the effects of CFRL on CFs, mCFs were treated with oe-CFRL or negative control for *in vitro* functional assays. A scratch wound-healing assay was applied to investigate the effect on cell migration, and the results showed that overexpressing CFRL markedly enhanced the motility of mCFs (Figures 2F and 2G). The proliferation of mCFs was quantified by CCK-8 analysis, which demonstrated that CFRL overexpression led to a significant increase in cell proliferation (Figure 2H). qRT-PCR and western Blot results also revealed that CFRL raised the expression of collagen type I alpha 1 chain (COL1A1) and alpha-smooth muscle actin (α -SMA), two biomarkers of CF activation (Figures 2I, 2J, and S8B).

Furthermore, we transfected mCFs with siRNAs targeting CFRL to silence it. RT-qPCR results showed the decreased expression of CFRL in mCFs (Figure S3A). In contrast to the effect of overexpression, compared with NC-transfected mCFs, si-CFRL transfected mCFs showed the decrease in cell viability, cell proliferation, and expression of fibrosis biomarkers (Figures 2F–2J), as well as the RNA and protein levels of CTGF and FN1 (Figures 2C–2E). To further verify that CTGF and FN1 were the functional target of CFRL, siRNAs targeting CTGF or FN1 were constructed and transfected into mCFs for knockdown (Figure S3B). CFRL was found to decrease dramatically with silencing CTGF or FN1, measuring by qRT-PCR (Figure 2K). All these data suggested that CFRL enhanced CF function by targeting both CTGF and FN1.

CFRL functions as a sponge for miR-3113-5p and miR-3473d

It has been shown that lncRNAs can act as miRNAs sponge to regulate downstream targets.^{11–13} The function of non-coding RNA, including lncRNA, has a close relationship with its subcellular location. FISH assay with a probe targeting the back-spliced junction of CFRL revealed the predominately cytoplasmic enrichment of CFRL in mCFs (Figure 3A). Therefore, we speculated that CFRL might be involved in cardiac fibrosis by acting as a ceRNA. lncRNAs and mRNA may share the same miRNAs according to the ceRNA theory.¹⁴ Therefore, we constructed a CFRL-miRNAs-CTGF/FN1 network through miRanda prediction, and found that CFRL might function as a sponge for miR-3113-5p to target CTGF, also a sponge for miR-3473d to target FN1 (Figure S4).

To confirm CFRL could bind to miR-3113-5p/miR-3473d, we constructed luciferase reporters containing wild type and mutated putative binding sites of CFRL (Figure S5). Dual-luciferase reporter assays showed that the luciferase activities of CFRL wild type reporter were significantly reduced when transfected with miR-3113-5p/miR-3473d mimics compared with control reporter or mutated luciferase reporter (Figures 3B and 3C).

Next, we constructed biotin-labeled CFRL-specific probes and performed an experiment to test whether CFRL could pull down miR-3113-5p and miR-3473d. The qRT-PCR results demonstrated binding of CFRL to miR-3113-5p and miR-3473d (Figures 3D and 3E). Taken together these results suggested that CFRL interacts directly with miR-3113-5p and miR-3473d.

For further verification, we suppress CFRL by transfect siRNAs in mCFs, the RNA levels for both miR-3113-5p and miR-3473d were markedly increased (Figure 3F). Meanwhile, miR-3113-5p and miR-3473d overexpression or knockdown through their mimics or inhibitors (Figures S3C and S3D) significantly decreased or increased RNA levels of CFRL separately (Figure 3G). These results suggested that CFRL functioned as a molecular sponge for miR-3113-5p and miR-3473d in mCFs.

MiR-3113-5p and miR-3473d target CTGF and FN1 respectively

The bioinformatics analysis data also showed that the 3'-UTR of CTGF and FN1 contained potential binding sites for miR-3113-5p and miR-3473d (Figure 4A). To confirm CTGF/FN1 could be regulated by miR-3113-5p/miR-3473d, we also constructed luciferase reporters containing wild type and mutated putative binding sites of CTGF/FN1 3'-UTR (Figure S6). Results unveiled that miR-3113-5p/miR-3473d combined with CTGF/FN1, evidenced by the remarkable reduction of CTGF/FN1 3'-UTR wild type reporter transfected with miRNA mimics (Figure 4B). Furthermore, qRT-PCR analysis revealed that silencing miR-3113-5p with its inhibitors dramatically increased CTGF expression in mCFs, as did miR-3473d for FN1 (Figure 4C). Overexpression of miR-3113-5p and miR-3473d with their corresponding mimics reduced CTGF and FN1 RNA levels, respectively, in mCFs (Figure 4D). Western Blot further proved that the protein levels of CTGF and FN1 were modulated by miR-3113-5p and miR-3473d (Figure 4E and S8C). Conversely, silencing CTGF or FN1 through siRNAs increased miR-3113-5p or

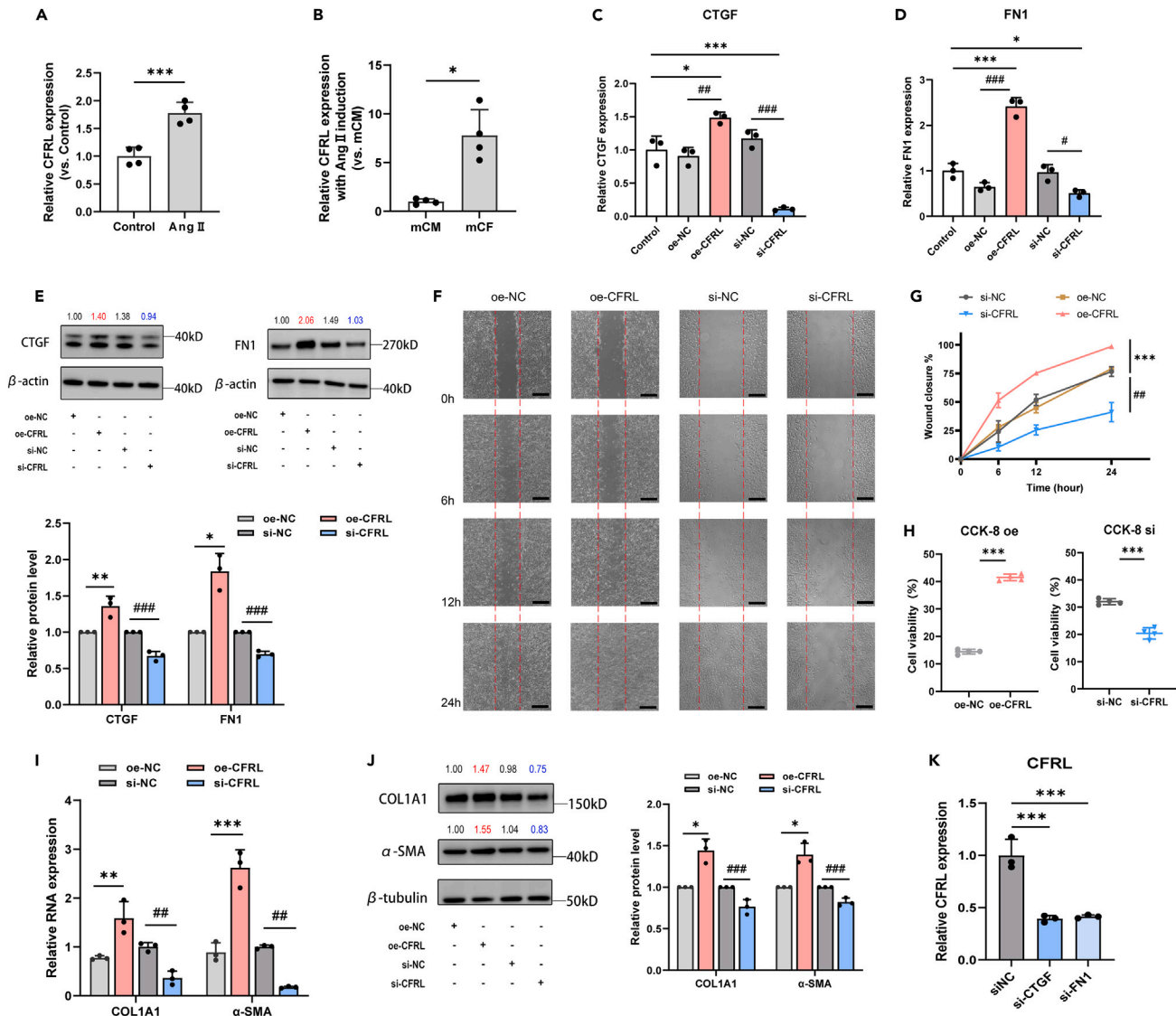


Figure 2. CFRL up-regulated CTGF and FN1 levels and increased cell viability and proliferation in mCFs

(A) CFRL was increased in mCFs after treatment with Ang II. n = 4 independent cell cultures. ***p < 0.001 vs. control.
 (B) CFRL expression in AngII-treated mCFs was higher than that in AngII-treated mCMs. n = 4. ***p < 0.001 vs. mCMs.
 (C and D) Overexpression of CFRL increased CTGF and FN1 expression, while the suppression had the opposite effect, as measured by qRT-PCR. n = 3 independent cell cultures. *p < 0.05, ***p < 0.001 vs. control, #p < 0.05, ##p < 0.01, ###p < 0.001 vs. oe- or si-negative control (NC).
 (E) Western blot analysis showing that knockdown of CFRL alleviated CTGF and FN1 protein expression, which overexpression intensified; β-actin served as a loading control, *p < 0.05, **p < 0.01 vs. oe-NC, ###p < 0.001 vs. si-NC.
 (F and G) Overexpressing CFRL enhanced cell migration of mCFs, as proved by wound-healing assay. Wound area was counted using ImageJ and used to calculate the wound closure rate (%) at 24 h post scratching (G). Scale bar, 200 μm. n = 3 independent cell cultures. ***p < 0.001 vs. oe-NC, ##p < 0.01 vs. si-NC.
 (H) CCK-8 for the assessment of proliferation, showing that CFRL overexpression led to an increase in cell viability and proliferation. n = 4 independent cell cultures, ***p < 0.001 vs. oe- or si-NC.
 (I) qRT-PCR analysis showing that overexpressing CFRL raised the RNA level of COL1A1 and α-SMA. n = 3. **p < 0.01 vs. oe-NC, ##p < 0.01, ###p < 0.001 vs. si-NC.
 (J) CFRL overexpression promoted COL1A1 and α-SMA protein expression, as measured by western blot; β-tubulin served as a loading control, *p < 0.05 vs. oe-NC, ###p < 0.001 vs. si-NC.
 (K) Silencing CTGF or FN1 decreased CFRL expression. n = 3. *p < 0.05, ***p < 0.001 vs. si-NC.

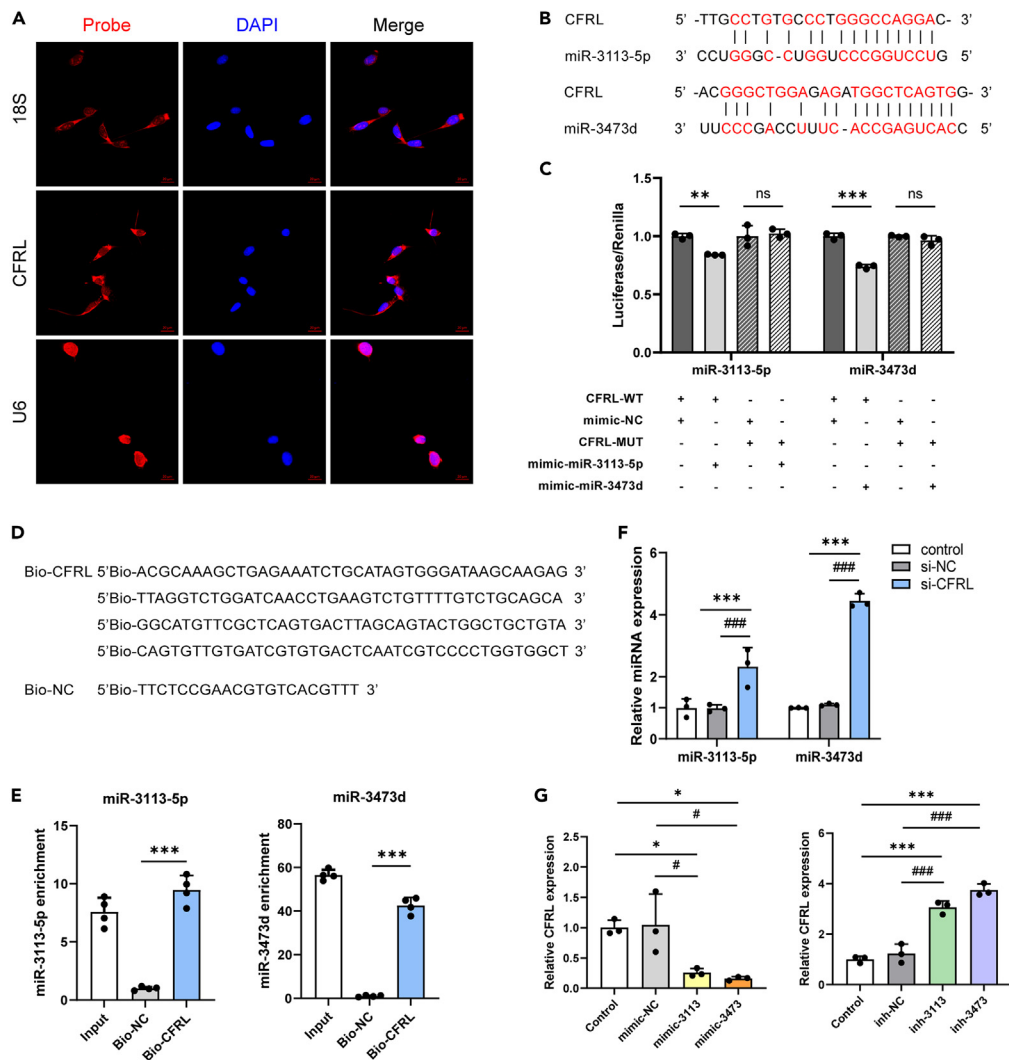


Figure 3. Interaction between CFRL and miR-3113-5p/miR-3473d

(A) Localization of CFRL in mCFs was detected by RNA-FISH analysis (Original magnification, $\times 500$, Scale bar, 20 μm). 18S and U6 served as a positive control for cytoplasmic and nuclear fractions, respectively. The nuclei were stained with DAPI. Fluorescent staining: DAPI (blue), CFRL (red), 18S (red), U6 (red).

(B) The predicted binding sites of miR-3113-5p and miR-3473d with CFRL. The complementary base pairs in CFRL are outlined in red.

(C) Luciferase assay results to validate the direct interaction of miR-3113-5p and miR-3473d with CFRL. $n = 3$ in each group. * $p < 0.05$, *** $p < 0.001$. "ns" meant not statistically significant. WT, wild type; MUT, mutant binding site.

(D and E) MiR-3113-5p and miR-3473d were pulled down by CFRL probe, and the expression of miR-3113-5p and miR-3473d were analyzed by qRT-PCR. $n = 4$. *** $p < 0.001$ vs. Bio-NC.

(F) CFRL knockdown by the specific siRNA upregulated miR-3113-5p and miR-3473d in mCFs.

(G) Overexpressing and silencing miR-3113-5p/miR-3473d through their mimics or inhibitors, respectively, CFRL expression was correspondingly decreased and increased. $n = 3$ independent cell cultures. * $p < 0.05$, ** $p < 0.01$, *** $p < 0.001$ vs. control, # $p < 0.05$, ## $p < 0.01$, ### $p < 0.001$ vs. NC.

miR-3473d expression accordingly (Figure 4F). The results of functional assays including scratch wound-healing assay (Figures 4G and 4H) and CCK-8 cell viability assay (Figure 4I) demonstrated that miR-3113-5p and miR-3473d knockdown enhanced the cell viability and proliferation in mCFs, while overexpression have the opposite effect. Further transfecting mCFs with miRNA inhibitors and si-CTGF or FN1 together, qRT-PCR showed that CTGF or FN1 knockdown reversed the pro-fibrotic effects of silencing miR-3113-5p or miR-3473d (Figures 4J–4L). These results revealed that CTGF/FN1 was the direct and functional target of miR-3113-5p/miR-3473d.

CFRL facilitates cell activity via the miR-3113-5p/CTGF & miR-3473d/FN1 axis in mCFs

These results together suggested that CFRL could bind to miR-3113-5p and miR-3473d, and CTGF/FN1 could be regulated by miR-3113-5p/miR-3473d and CFRL. In order to further confirm that CFRL could contribute to cardiac fibrosis via the miR-3113-5p/CTGF & miR-3473d/FN1

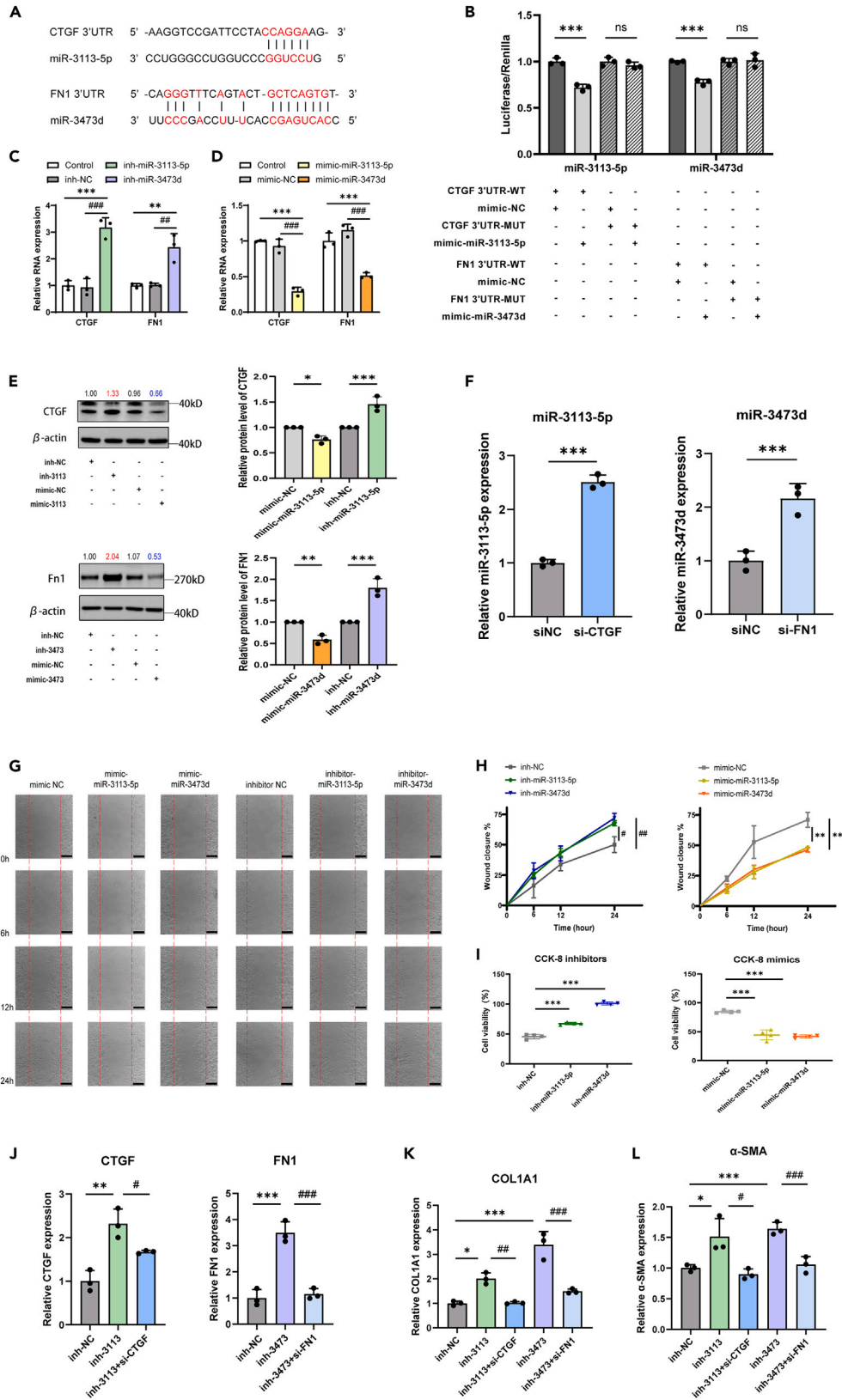


Figure 4. miR-3113-5p and miR-3473d targeted CTGF and FN1, respectively, modulating cell viability and proliferation in MCFs

(A) Sequence alignment showing complementarity of miR-3113-5p and CTGF 3'UTR, as well as miR-3473d and FN1 3'UTR. The matched base pairs are outlined in red.

(B) Luciferase assay showing validation of the binding of miR-3113-5p and CTGF 3'UTR, also miR-3473d and FN1 3'UTR. n = 3 in each group. "ns" meant not statistically significant. WT, wild type; MUT, mutant binding site.

(C and D) Transfection of miR-3113-5p and miR-3473d inhibitors increased CTGF and FN1 expression, respectively, while transfecting mimics reduced the RNA levels of them, as measured by qRT-PCR. n = 3 independent cell cultures. **p < 0.01, ***p < 0.001 vs. control, ##p < 0.01, ###p < 0.001 vs. NC.

(E) miR-3113-5p/miR-3473d mimics and inhibitors downregulated and upregulated the expression of corresponding targets, respectively, as measured by western blot, *p < 0.05, **p < 0.01, ***p < 0.001 vs. mimic- or inh-NC.

(F) qRT-PCR showing that transfection of CTGF and FN1 siRNAs increased miR-3113-5p and miR-3473d expression, respectively. n = 3. ***p < 0.001 vs. si-NC.

(G) Wound-healing assay showing that transfection of mi-3113-5p/miR-3473d mimics attenuated cell migration of mCFs. Scale bar, 200 μ m.

(H) Wound closure rate was calculated the at 24 h post scratching. n = 3 independent cell cultures. **p < 0.01 vs. mimic-NC, #p < 0.05, ##p < 0.01 vs. inh-NC.

(I–L) CCK-8 assay showing a decline in cell viability and proliferation with miR-3113-5p/miR-3473d overexpression. n = 4 independent cell cultures. ***p < 0.001 vs. mimic-NC or inh-NC. Suppressing CTGF or FN1 in miR-3113-5p or miR-3473d-downregulated mCFs partly decreased the levels of CTGF or FN1 (J), COL1A1 (K) and α -SMA (L), as measured by qRT-PCR. n = 3. *p < 0.05, **p < 0.01, ***p < 0.001 vs. inh-NC. #p < 0.05, ##p < 0.01, ###p < 0.001 vs. inh-3113/3473.

axis, we transfected mCFs with miRNA inhibitors and si-CFRL at the same time. Results demonstrated that suppressing miR-3113-5p or miR-3473d in CFRL-downregulated mCFs could rescue the inhibitory effects of CFRL knockdown on RNA and protein levels of CTGF and FN1. On the contrary, compared with the oe-CFRL transfects, the co-transfection of oe-CFRL and miR-3113-5p/miR-3473d mimics showed lower RNA and protein levels of CTGF and FN1 (Figures 5A and 5B).

Meanwhile, co-transfection of miR-3113-5p/miR-3473d inhibitors and si-CFRL partly promoted cell activity in mCFs, compared with si-CFRL group. In contrast, miR-3113-5p or miR-3473d overexpression eliminated the promotion of CFRL on cell migration and proliferation in mCFs (Figures 5C–5E). Co-transfection of miR-3113-5p/miR-3473d inhibitors and si-CTGF/FN1 was also conducted. Results showed that silencing CTGF or FN1 relieved the overexpression of CFRL aroused by silencing miR-3113-5p/miR-3473d (Figure 5F). These results further discovered that CFRL served as a molecular sponge for miR-3113-5p or miR-3473d and facilitated cell activity via the miR-3113-5p/CTGF & miR-3473d/FN1 axis in mCFs.

Silencing of CFRL mitigates cardiac fibrosis and protects cardiac function in mice subjected to TAC

To explore the biological functions of CFRL *in vivo*, we treated the mice with the overexpressing construction and siRNA of CFRL via tail vein injection to perform CFRL overexpression and knockdown. At 2 weeks after injection, echocardiography was taken to assess the cardiac function. CFRL-overexpressed TAC mice showed decreased ejection fraction (EF%) and fraction shortening (FS%) (Figure 6A). Atrial natriuretic peptide (ANP) and brain natriuretic peptide (BNP) expression also increased, as measured by qRT-PCR (Figure 6B). Images of mice hearts showing that the injection of oe-CFRL aggravated cardiac hypertrophy (Figure 6C). These results indicated that CFRL overexpression aggravated cardiac impairment. Sirius Red staining analysis further proved that oe-CFRL group suffered from worse cardiac fibrosis induced by TAC, showing increased interstitial fibrosis area (Figures 6D and S7). The expression of fibrosis-related genes, COL1A1 and α -SMA, was also increased (Figure 6E). Meanwhile, qRT-PCR and western blot results revealed the up-regulated RNA and protein levels of CTGF and FN1 (Figures 6F, 6G, and S8D). The expression of miR-3113-5p and miR-3473d also decreased (Figure 6H). Taken together, these results verified the pro-fibrotic role and underlying mechanism of CFRL *in vivo*.

On the contrary, compared with TAC-induced mice, CFRL silencing group showed restored cardiac function, evidenced by higher EF (%) / FS (%) (Figure 6A), lower RNA levels of ANP and BNP (Figure 6B) and less hypertrophic hearts (Figure 6C). Suppressing CFRL also mitigated cardiac fibrosis, as proved by Sirius Red staining analysis (Figure 6D) and reduction of COL1A1 and α -SMA (Figure 6E). qRT-PCR and western blot also showed a decline in RNA and protein levels of CTGF and FN1 (Figures 6F and 6G), as well as increased miR-3113-5p and miR-3473d (Figure 6H). These results suggested that CFRL knockdown was able to mitigate cardiac fibrosis and protect cardiac function. Therefore, interfering with CFRL expression might be considered as a new strategy for the management of cardiac fibrosis.

DISCUSSION

In this study, we described an up-regulated lncRNA in TAC-induced mice model, which was named CFRL. CFRL could target both CTGF and FN1, two significant fibrosis genes, by acting as a ceRNA of miR-3113-5p and miR3473d to promote fibrosis progress. Therefore, we discovered a new upstream regulator of cardiac fibrosis and its underlying mechanism. Moreover, CFRL knockdown *in vivo* remarkably ameliorated fibrosis and cardiac function, which presented a new insight into the therapeutic strategies of cardiac fibrosis.

lncRNAs are transcripts of >200 nucleotides in length with a higher total quantity than protein-coding genes,^{15,16} and exhibit more highly specific expression patterns than mRNAs.¹⁷ Studies have revealed that lncRNAs may be crucial in a variety of physiological and pathological processes.¹⁸ In our study, we first discovered the up-regulation of CFRL in the TAC mice through whole transcriptome RNA-sequencing and verified by experiments *in vivo* and *in vitro*. To further reveal the underlying mechanism, we constructed the co-expression network to predicted and then confirmed that CFRL targets both CTGF and FN1, having a critical role in cardiac fibrosis. So far, a number of lncRNAs have been proved to be involved in the progress of cardiac fibrosis. lncRNA PCFL, as an illustration, was demonstrated to promote cardiac fibrosis via miR-378/GRB2 pathway.¹⁹ However, most of these lncRNAs are only found to regulate single gene, and the function of some downstream

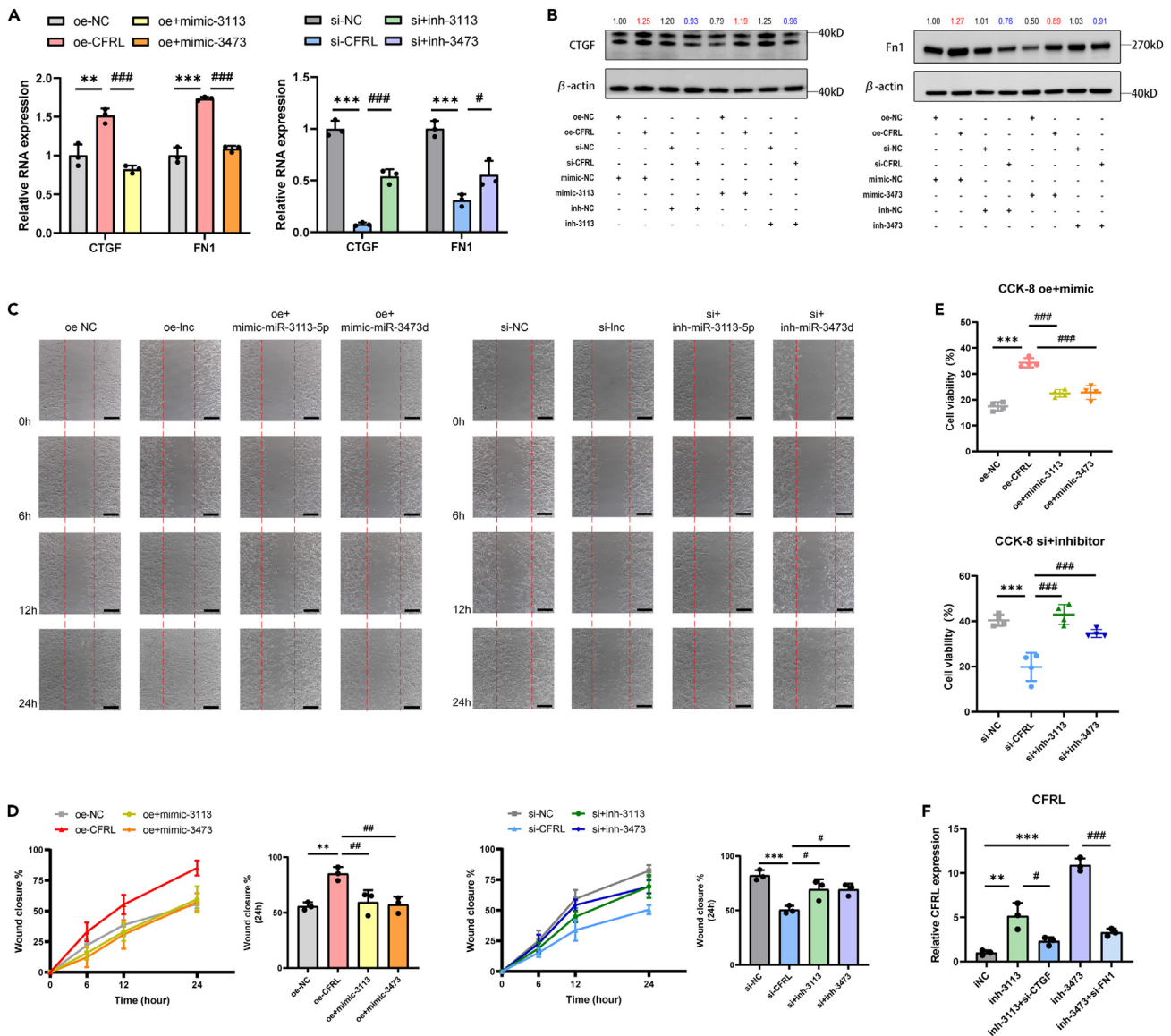


Figure 5. CFRL functioned via the miR-3113-5p/CTGF & miR-3473d/FN1 axis in mCFs

(A) qRT-PCR showing that suppressing miR-3113-5p/miR-3473d in CFRL-downregulated mCFs partly increased the levels of CTGF/FN1, and overexpressing miR-3113-5p/miR-3473d alleviated the CTGF/FN1 upregulation induced by CFRL overexpression. n = 3 independent cell cultures. **p < 0.01, ***p < 0.001 vs. oe- or si-NC, #p < 0.05, ###p < 0.001 vs. oe- or si-CFRL.

(B) Western blot showing that co-transfection of miRNA mimics and oe-CFRL partly reversed the effect of CFRL on CTGF and FN1, as well as miRNA inhibitors and si-CFRL.

(C and D) Wound-healing assay and wound closure rate at 24 h demonstrated that up-regulating miR-3113-5p/miR-3473d in oe-CFRL transfected mCFs rescued the promotion of CFRL on cell migration. In contrast, co-transfection of miRNA inhibitors and siRNAs promoted cell migration, compared with si-CFRL group. Scale bar, 200 μ m. n = 3 independent cell cultures. **p < 0.01, ***p < 0.001 vs. oe- or si-NC, #p < 0.05, ##p < 0.01 vs. oe- or si-CFRL.

(E) CCK-8 analysis further quantified the cell viability and proliferation of mCFs. n = 4 independent cell cultures. ***p < 0.001 vs. oe- or si-NC, ###p < 0.001 vs. oe- or si-CFRL.

(F) As measured by qRT-PCR, suppressing CTGF/FN1 in miR-3113-5p/miR-3473d-downregulated mCFs partly decreased the levels of CFRL. n = 3. **p < 0.01, ***p < 0.001 vs. inh-NC, #p < 0.05, ###p < 0.001 vs. inh-3113/3473.

target genes have not been well-established. Therefore, our study characterized an lncRNA that target both two well-known fibrosis genes, which might play a more important role in cardiac fibrosis.

In mechanism, lncRNAs could act as molecular guides and scaffolds to interact with protein complexes or guide chromatin-modifying complexes to target genomic DNA loci.²⁰ More importantly, accumulating evidence has shown that lncRNAs participate in cardiovascular

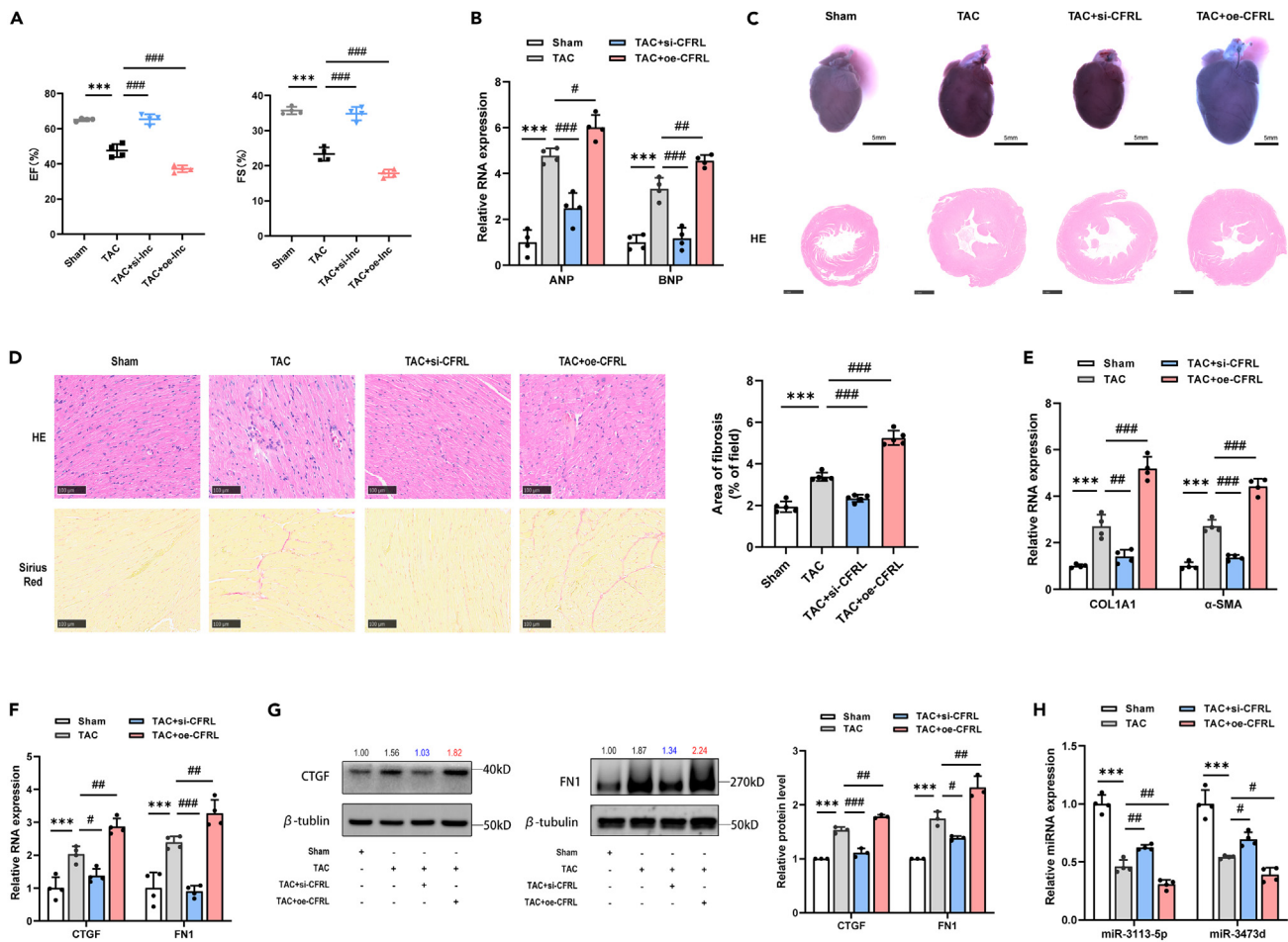


Figure 6. CFRL aggravated cardiac fibrosis and cardiac impairment in vivo

(A and B) Overexpression of CFRL intensified impaired cardiac function in TAC induced mice, while suppressing CFRL alleviated it, evidenced by ejection fraction (EF%) and fraction shortening (FS%) measured by echocardiography (A) and expression of ANP and BNP measured by qRT-PCR (B). $n = 4$ mice per group. *** $p < 0.001$ vs. Sham, # $p < 0.05$, ## $p < 0.01$, ### $p < 0.001$ vs. TAC.

(C) Representative images of mice hearts showing that the injection of si-CFRL alleviated TAC-induced cardiac hypertrophy, while oe-CFRL aggravated it.

(D–H) Representative images of HE and Sirius Red-stained LV tissue of TAC mice after injection of oe- and si-CFRL. Scale bar, 100 μ m. Quantification of the fibrotic area showed using ImageJ. $n = 5$. *** $p < 0.001$ vs. Sham, ### $p < 0.001$ vs. TAC. qRT-PCR and western blot analysis indicated that CFRL promoted the expression of fibrosis-related genes, including COL1A1 and α -SMA (E), and increased the RNA (F) and protein (G) levels of CTGF/FN1, and decreased the expression of miR-3113-5p/miR-3473d (H). $n = 4$ mice per group. *** $p < 0.001$ vs. Sham, # $p < 0.05$, ## $p < 0.01$, ### $p < 0.001$ vs. TAC.

diseases by acting as ceRNA, where RNA transcripts with the same binding sites are natural decoys in miRNAs activity by competing for common miRNAs.¹⁴ Similarly, in our study, CFRL was predicted to have potential binding sites and could sponge both miR-3113-5p and miR-3473d, which was subsequently proved by dual-luciferase reporter assay. Further gain- and loss-of function experiment *in vitro* confirmed these results.

MicroRNAs (miRNAs) are single-stranded transcripts with sizes of about 22 nucleotides which repress the expression of mRNA targets by promoting translational repression and mRNA degradation.^{16,21,22} In recent years, many studies have demonstrated that microRNAs (miRNAs) might play an important role in cardiac fibrosis. To our knowledge, there are few research on the function and mechanism of miR-3473d, while miR-3113-5p has been reported to be upregulated and participated in cardiac I/R injury and sudden cardiac death (SCD) cases.^{23,24} However, we found downregulation of miR-3113-5p and miR-3473d in TAC mice, illustrating their novel role in fibrosis. Cell viability and migration of mCF was significantly promoted by suppressing miR-3113-5p or miR-3473d, further proving that both of them are crucial in cardiac fibrosis. Moreover, the complete ceRNA network was established and its impact on fibrosis was confirmed by the CCK-8 assay and wound healing assay in mCFs. Overexpression of CFRL and knockdown of miR-3113-5p/miR3473d promoted cardiac fibrosis, as proved by the facilitated cell activity of mCFs. Taken together, we demonstrated that CFRL aggravated cardiac fibrosis by modulating both miR-3113-5p/CTGF and miR-3473d/FN1 axis. These results further illustrated the underlying mechanism of CFRL regulating both two vital fibrotic genes and provided a theoretical basis for potential therapeutic use.

Furthermore, the function of CFRL *in vivo* was evaluated by CFRL overexpression and knockdown in TAC mice. The result of Sirius Red staining and echocardiography further proved that CFRL promoted cardiac fibrosis and worsen cardiac function. Moreover, suppressing CFRL in TAC mice could dramatically alleviate fibrosis and improve cardiac function. Since knockdown of ncRNA expression has proved to be easy using chemically engineered antisense oligonucleotides, or siRNA-mediated approaches,²⁵ our study presents a novel and potential target for the treatment of cardiac fibrosis. Previous studies have also discovered that the overexpression of protective lncRNA or knockdown of culprit lncRNA *in vivo* could mitigate fibrosis in animal models. However, most of them were found to only target a single pathway, while CFRL regulate both miR-3113-5p/CTGF and miR-3473d/FN1 axis. CTGF and FN1 have been proved to play an important role in cardiac fibrosis through promoting cell proliferation, motility, adhesion and matrix turnover,^{26,27} and suppressing CTGF or FN1 could alleviate cardiac fibrosis.²⁸ When it comes to anti-fibrotic drugs, numerous small molecules or compounds are currently in clinical trials for fibrosis, but few for cardiac fibrosis.²⁹ Pamrevlumab, a kind of anti-fibrotic drug targeting CTGF,³⁰ has showed promise as a safe and effective treatment,³¹ but in the field of idiopathic pulmonary fibrosis. Besides, there has been few anti-fibrotic drug targeting FN1 up to now. Therefore, interfering with CFRL expression may be considered as a new strategy for the prevention and treatment of cardiac fibrosis and associated pathological processes.

In brief, our research revealed that CFRL is a pro-fibrotic lncRNA stimulating cardiac fibrosis by competitively binding miR-3113-5p and miR-3473d thus targeting both CTGF and FN1. In a series of *in vitro* and *in vivo* experiments, we uncovered the characters of CFRL and miR-3113-5p/miR-3473d in cardiac fibrosis and clarified their regulatory interactions. These results suggest that preventing CFRL expression may be a new approach to treating and preventing cardiac fibrosis and HF.

Limitations of the study

Our study characterized a new critical fibrotic lncRNA and provided new mechanism of cardiac fibrosis. However, some limitations should be noted. First, lncRNAs lack the high interspecies conservation³² and the full length of CFRL is also poorly conserved. It is possible that the lncRNAs between human and mouse are conserved at the structural level.³³ Therefore, further thorough research could be conducted to find the human homologue for CFRL, from several conservation dimensions including the sequence, structure, function, and expression from syntenic loci dimensions. Second, TAC model was used to mimic cardiac fibrosis and HF *in vivo* experiments. However, there were several models of cardiac fibrosis, and CFRL expression should also be detected in LV tissues of other models including AngII infusion and two-kidneys-one-clip. Besides, the attempt to overexpress miR-3113-5p/miR-3473d *in vivo* experiments failed, so further research was needed. Third, the role of CFRL in hypertrophy remained unclear. Despite the enrichment of CFRL in mCFs rather than in mCMs, histological analysis demonstrated that the injection of si-CFRL alleviated TAC-induced cardiac hypertrophy, while oe-CFRL aggravated it. Last, there might be other possible target genes of CFRL besides CTGF and FN1. Therefore, further study was required.

STAR★METHODS

Detailed methods are provided in the online version of this paper and include the following:

- [KEY RESOURCES TABLE](#)
- [RESOURCE AVAILABILITY](#)
 - Lead contact
 - Materials availability
 - Data and code availability
- [EXPERIMENTAL MODEL AND STUDY PARTICIPANT DETAILS](#)
 - Animals
 - Cells
- [METHOD DETAILS](#)
 - Histological analysis
 - RNA fluorescence *in situ* hybridization (FISH)
 - Dual luciferase assay
 - Wound-healing assay
 - CCK-8 cell viability assay
 - Quantitative reverse transcription-PCR (qRT-PCR)
 - Western Blot
- [QUANTIFICATION AND STATISTICAL ANALYSIS](#)

ACKNOWLEDGMENTS

This work was supported by the National Natural Science Foundation of China (grant number 82172101, 82072081), the Major Clinical Research Youth Project of Shanghai Hospital Development Center (grant number SHDC2020CR4093), the Emerging Advanced Technology Joint Research of Shanghai Hospital Development Center (grant number SHDC12021106), the Science and Technology Development Fund of Shanghai Pudong New Area (grant number PKJ2021-44), the General Program of Shanghai Health Committee (grant number 202040337) and Shanghai Jude Charitable Foundation.

AUTHOR CONTRIBUTIONS

Conceptualization, Y.C., B.S., Zijie Zhou, J.Z. and X.H.; methodology, Y.C., B.S., Zijie Zhou, B.C., X.Z., C.L., K.L., Zhongqun Zhu, J.Z. and X.H.; formal analysis, Y.C. and X.H.; investigation, Y.C., B.S., Zijie Zhou, B.C., and X.H.; resources, Y.C., B.S., Zijie Zhou, J.Z. and X.H.; writing (original draft), Y.C. and X.H.; writing (review and editing), Y.C., B.S., Zijie Zhou, J.Z. and X.H.; visualization, Y.C. and X.H.; supervision, J.Z. and X.H.

DECLARATION OF INTERESTS

The authors declare no competing interests.

INCLUSION AND DIVERSITY

We support inclusive, diverse, and equitable conduct of research.

Received: March 29, 2023

Revised: July 13, 2023

Accepted: September 21, 2023

Published: September 25, 2023

REFERENCES

- Liu, H., Fan, P., Jin, F., Huang, G., Guo, X., and Xu, F. (2022). Dynamic and static biomechanical traits of cardiac fibrosis. *Front. Bioeng. Biotechnol.* 10, 1042030. <https://doi.org/10.3389/fbioe.2022.1042030>.
- Talman, V., and Ruskoaho, H. (2016). Cardiac fibrosis in myocardial infarction—from repair and remodeling to regeneration. *Cell Tissue Res.* 365, 563–581. <https://doi.org/10.1007/s00441-016-2431-9>.
- Gyöngyösi, M., Winkler, J., Ramos, I., Do, Q.T., Firat, H., McDonald, K., González, A., Thum, T., Diez, J., Jaisser, F., et al. (2017). Myocardial fibrosis: biomedical research from bench to bedside. *Eur. J. Heart Fail.* 19, 177–191. <https://doi.org/10.1002/ehfj.696>.
- Kong, P., Christia, P., and Frangogiannis, N.G. (2014). The pathogenesis of cardiac fibrosis. *Cell. Mol. Life Sci.* 71, 549–574. <https://doi.org/10.1007/s00018-013-1349-6>.
- Chatzifrangkeskou, M., Le Dour, C., Wu, W., Morrow, J.P., Joseph, L.C., Beuvin, M., Sera, F., Homma, S., Vignier, N., Mougnot, N., et al. (2016). ERK1/2 directly acts on CTGF/CCN2 expression to mediate myocardial fibrosis in cardiomyopathy caused by mutations in the lamin A/C gene. *Hum. Mol. Genet.* 25, 2220–2233. <https://doi.org/10.1093/hmg/ddw090>.
- Valiente-Alandi, I., Potter, S.J., Salvador, A.M., Schafer, A.E., Schips, T., Carrillo-Salinas, F., Gibson, A.M., Nieman, M.L., Perkins, C., Sargent, M.A., et al. (2018). Inhibiting Fibronectin Attenuates Fibrosis and Improves Cardiac Function in a Model of Heart Failure. *Circulation* 138, 1236–1252. <https://doi.org/10.1161/circulationaha.118.034609>.
- Qi, X., Zhang, D.H., Wu, N., Xiao, J.H., Wang, X., and Ma, W. (2015). ceRNA in cancer: possible functions and clinical implications. *J. Med. Genet.* 52, 710–718. <https://doi.org/10.1136/jmedgenet-2015-103334>.
- Chen, S., Zhang, Y., Ding, X., and Li, W. (2022). Identification of lncRNA/circRNA-miRNA-mRNA ceRNA Network as Biomarkers for Hepatocellular Carcinoma. *Front. Genet.* 13, 838869. <https://doi.org/10.3389/fgene.2022.838869>.
- Liang, H., Pan, Z., Zhao, X., Liu, L., Sun, J., Su, X., Xu, C., Zhou, Y., Zhao, D., Xu, B., et al. (2018). LncRNA PFL contributes to cardiac fibrosis by acting as a competing endogenous RNA of let-7d. *Theranostics* 8, 1180–1194. <https://doi.org/10.7150/tno.20846>.
- Jaé, N., and Dimmeler, S. (2020). Noncoding RNAs in Vascular Diseases. *Circ. Res.* 126, 1127–1145. <https://doi.org/10.1161/circresaha.119.315938>.
- Karagkouni, D., Karavangeli, A., Paraskevopoulou, M.D., and Hatzigeorgiou, A.G. (2021). Characterizing miRNA-lncRNA Interplay. *Methods Mol. Biol.* 2372, 243–262. https://doi.org/10.1007/978-1-0716-1697-0_21.
- Rashid, F., Shah, A., and Shan, G. (2016). Long Non-coding RNAs in the Cytoplasm. *Dev. Reprod. Biol.* 14, 73–80. <https://doi.org/10.1016/j.gpb.2016.03.005>.
- Zhang, K., Shi, Z.M., Chang, Y.N., Hu, Z.M., Qi, H.X., and Hong, W. (2014). The ways of action of long non-coding RNAs in cytoplasm and nucleus. *Gene* 547, 1–9. <https://doi.org/10.1016/j.gene.2014.06.043>.
- Salmena, L., Poliseno, L., Tay, Y., Kats, L., and Pandolfi, P.P. (2011). A ceRNA hypothesis: the Rosetta Stone of a hidden RNA language? *Cell* 146, 353–358. <https://doi.org/10.1016/j.cell.2011.07.014>.
- Djebali, S., Davis, C.A., Merkel, A., Dobin, A., Lassmann, T., Mortazavi, A., Tanzer, A., Lagarde, J., Lin, W., Schlesinger, F., et al. (2012). Landscape of transcription in human cells. *Nature* 489, 101–108. <https://doi.org/10.1038/nature11233>.
- Ghafouri-Fard, S., Abak, A., Talebi, S.F., Shoorei, H., Branicki, W., Taheri, M., and Akbari Dilmaghani, N. (2021). Role of miRNA and lncRNAs in organ fibrosis and aging. *Biomed. Pharmacother.* 143, 112132. <https://doi.org/10.1016/j.biopha.2021.112132>.
- Quinn, J.J., and Chang, H.Y. (2016). Unique features of long non-coding RNA biogenesis and function. *Nat. Rev. Genet.* 17, 47–62. <https://doi.org/10.1038/nrg.2015.10>.
- Wu, T., and Du, Y. (2017). LncRNAs: From Basic Research to Medical Application. *Int. J. Biol. Sci.* 13, 295–307. <https://doi.org/10.7150/ijbs.16968>.
- Sun, F., Zhuang, Y., Zhu, H., Wu, H., Li, D., Zhan, L., Yang, W., Yuan, Y., Xie, Y., Yang, S., et al. (2019). LncRNA PCFL promotes cardiac fibrosis via miR-378/GRB2 pathway following myocardial infarction. *J. Mol. Cell. Cardiol.* 133, 188–198. <https://doi.org/10.1016/j.yjmcc.2019.06.011>.
- Archer, K., Broskova, Z., Bayoumi, A.S., Teoh, J.P., Davila, A., Tang, Y., Su, H., and Kim, I.M. (2015). Long Non-Coding RNAs as Master Regulators in Cardiovascular Diseases. *Int. J. Mol. Sci.* 16, 23651–23667. <https://doi.org/10.3390/ijms161023651>.
- Iwakawa, H.O., and Tomari, Y. (2015). The Functions of MicroRNAs: mRNA Decay and Translational Repression. *Trends Cell Biol.* 25, 651–665. <https://doi.org/10.1016/j.tcb.2015.07.011>.
- Huntzinger, E., and Izaurralde, E. (2011). Gene silencing by microRNAs: contributions of translational repression and mRNA decay. *Nat. Rev. Genet.* 12, 99–110. <https://doi.org/10.1038/nrg2936>.
- Chen, Y., Ye, X., and Yan, F. (2019). MicroRNA 3113-5p is a novel marker for early cardiac ischemia/reperfusion injury. *Diagn. Pathol.* 14, 121. <https://doi.org/10.1186/s13000-019-0894-1>.
- Yan, F., Chen, Y., Ye, X., Zhang, F., Wang, S., Zhang, L., and Luo, X. (2021). miR-3113-5p, miR-223-3p, miR-133a-3p, and miR-499a-5p are sensitive biomarkers to diagnose sudden cardiac death. *Diagn. Pathol.* 16, 67. <https://doi.org/10.1186/s13000-021-01127-x>.
- Morris, K.V., and Mattick, J.S. (2014). The rise of regulatory RNA. *Nat. Rev. Genet.* 15, 423–437. <https://doi.org/10.1038/nrg3722>.
- Leask, A. (2010). Potential therapeutic targets for cardiac fibrosis: TGFbeta, angiotensin, endothelin, CCN2, and PDGF, partners in fibroblast activation. *Circ. Res.* 106, 1675–1680. <https://doi.org/10.1161/circresaha.110.217737>.
- Maruyama, K., and Imanaka-Yoshida, K. (2022). The Pathogenesis of Cardiac Fibrosis: A Review of Recent Progress. *Int. J. Mol. Sci.* 23, 2617. <https://doi.org/10.3390/ijms23052617>.
- Park, S., Nguyen, N.B., Pezhouman, A., and Ardehali, R. (2019). Cardiac fibrosis: potential therapeutic targets. *Transl. Res.* 209, 121–137. <https://doi.org/10.1016/j.trsl.2019.03.001>.
- Zhao, M., Wang, L., Wang, M., Zhou, S., Lu, Y., Cui, H., Racaneli, A.C., Zhang, L., Ye, T., Ding, B., et al. (2022). Targeting fibrosis, mechanisms and clinical trials. *Signal*

- Transduct. Targeted Ther. 7, 206. <https://doi.org/10.1038/s41392-022-01070-3>.
30. Lipson, K.E., Wong, C., Teng, Y., and Spong, S. (2012). CTGF is a central mediator of tissue remodeling and fibrosis and its inhibition can reverse the process of fibrosis. *Fibrogenesis Tissue Repair* 5, S24. <https://doi.org/10.1186/1755-1536-5-s1-s24>.
 31. Richeldi, L., Fernández Pérez, E.R., Costabel, U., Albera, C., Lederer, D.J., Flaherty, K.R., Ettinger, N., Perez, R., Scholand, M.B., Goldin, J., et al. (2020). Pamrevlumab, an anti-connective tissue growth factor therapy, for idiopathic pulmonary fibrosis (PRAISE): a phase 2, randomised, double-blind, placebo-controlled trial. *Lancet Respir. Med.* 8, 25–33. [https://doi.org/10.1016/s2213-2600\(19\)30262-0](https://doi.org/10.1016/s2213-2600(19)30262-0).
 32. Pang, K.C., Frith, M.C., and Mattick, J.S. (2006). Rapid evolution of noncoding RNAs: lack of conservation does not mean lack of function. *Trends Genet.* 22, 1–5. <https://doi.org/10.1016/j.tig.2005.10.003>.
 33. Torarinsson, E., Sawera, M., Havgaard, J.H., Fredholm, M., and Gorodkin, J. (2006). Thousands of corresponding human and mouse genomic regions unalignable in primary sequence contain common RNA structure. *Genome Res.* 16, 885–889. <https://doi.org/10.1101/gr.5226606>.

STAR★METHODS

KEY RESOURCES TABLE

REAGENT or RESOURCE	SOURCE	IDENTIFIER
Antibodies		
Rabbit monoclonal anti-CTGF	Abmart	Cat#TD7091S; RRID: AB_3065183
Rabbit polyclonal anti-FN1	absin	Cat#abs117932; RRID: AB_3065184
Rabbit monoclonal anti- β -actin	cell signaling technology	Cat#4967; RRID: AB_330288
Rabbit monoclonal anti- β -tubulin	cell signaling technology	Cat#2146; RRID: AB_2210545
Goat anti-Rabbit IgG (H + L) Secondary Antibody, HRP	Invitrogen	Cat#31460; RRID: AB_228341
Bacterial and virus strains		
m-CFRL-CBH-GFP Adenovirus	Hanyin Biotechnology	N/A
Chemicals, peptides, and recombinant proteins		
AngII	Sigma	CAS No. 4474-91-3
Critical commercial assays		
riboFECT™ CP Transfection Kit	RiboBio	Cat#C10511-05
BaseScope™ Detection Reagent Kit	ACD	Cat#323700
Dual-Luciferase Assay kit	Promega	Cat#E1910
Deposited data		
RNA-seq data	This paper; GEO	GSE228199
original data and western blot images	This paper; Mendeley Data	https://doi.org/10.17632/s64m3h4db5.1
Experimental models: Cell lines		
primary mouse cardiac fibroblasts (mCFs)	This paper	N/A
Experimental models: Organisms/strains		
Mouse: C57BL/6	Shanghai Jihui Laboratory Animal Care Co.,Ltd.	N/A
Oligonucleotides		
CFRL		
Forward Primer: TGCTCGCAGTAGGTCCTCAC	Gene Tools	N/A
Reverse Primer: GAGGAGTTTCAGCCGTCAAGAAGTGC		N/A
GAPDH		
Forward Primer: CATCACTGCCACCCAGAAGA	Gene Tools	N/A
Reverse Primer: GCCAGTGAGTTTCCCGTTCA		N/A
miR-3113-5p and miR-3473d		
Bulge-Loop™ miR-3113-5p/miR3473d RT Primer	RiboBio	N/A
Bulge-Loop™ miR-3113-5p/miR3473d Forward Primer		N/A
Bulge-Loop™ miRNA Reverse Primer		N/A
U6		
Bulge-Loop™ U6 RT Primer	RiboBio	N/A
Bulge-Loop™ U6 Forward Primer		N/A
Bulge-Loop™ U6 Reverse Primer		N/A
Recombinant DNA		
Plasmid: CFRL	Hanyin Biotechnology	N/A

(Continued on next page)

Continued

REAGENT or RESOURCE	SOURCE	IDENTIFIER
Software and algorithms		
ImageJ	N/A	https://imagej.nih.gov/ij/
Graphpad Prism V9.0	N/A	https://www.graphpad.com/
miRanda	N/A	http://www.microrna.org/

RESOURCE AVAILABILITY

Lead contact

Further information and requests for resources and reagents should be directed to and will be fulfilled by the lead contact, Xiaomin He (mrxmhe@163.com).

Materials availability

This study did not generate new unique reagents.

Data and code availability

- The RNA-seq data have been deposited at GEO and are publicly available as of the date of publication. Accession numbers are listed in the [key resources table](#). Other original data and western blot images have been deposited at Mendeley and are publicly available as of the date of publication. The DOI is listed in the [key resources table](#).
- This paper does not report original code.
- Any additional information required to reanalyze the data reported in this paper is available from the [lead contact](#) upon request.

EXPERIMENTAL MODEL AND STUDY PARTICIPANT DETAILS

Animals

Male C57BL/6 mice (8 weeks old) (Jihui Laboratory Animal Care Co., Ltd., Shanghai, China) were used in the studies. The mice were housed under a 12 h light/dark cycle under pathogen-free conditions and with free access to standard mouse chow and tap water. The mice chosen for experiments had similar body weight and were allocated to each group by random. All experiments were carried out in accordance with the guidelines for Animal Experimentation of Shanghai Jiao Tong University School of Medicine and approved by the Ethic Committees of Shanghai Children's Medical Center, also conforming to the NRC Guide for the Care and Use of Laboratory Animals (2011, 8th ed.).

8-week age male C57BL/6 mice were anesthetized by avertin (250 mg/kg, IP). Then a small left second intercostal incision was made to open the chest cavity of mice and the aortic arch was exposed. Transverse aortic constriction (TAC) operation was then performed by ligating the aorta between the right innominate and left carotid arteries using a 27G needle tied with 6-0 silk suture. The needle was then removed, and a stenosis of the aorta was formed. The mice were put into cages for recovery after closing the chest. The sham-operated mice underwent the similar procedure except for leaving the 6-0 silk suture without ligation.

Mice were randomly divided into four groups: the sham-operated control group, the TAC group, the si-CFRL and oe-CFRL group. Four weeks after the TAC surgery, each mouse of the si- or oe-CFRL group was further treated with si-CFRL (10 nmol, designed by Ribobio, Guangzhou, China), or m-CFRL-CBH-GFP Adenovirus (2.30×10^{10} pfu, provided by Hanyin Biotechnology) twice a week via tail vein injection for 2 weeks. Then the mice underwent echocardiography to assess the cardiac function and morphometric changes. Then, the mice were euthanized, and the left ventricle (LV) tissue was collected for the RNA/protein and histological analyses.

Cells

Neomyt kit (NC-6031, Cellutron, USA) was used to obtain primary neonatal mouse cardiac fibroblasts (mCFs) from neonatal C57BL/6 mice. LV tissues from 10 C57BL/6 mice were harvested and first digested for 12 min in 10 mL of enzyme buffer for each time experiment. Then the supernatant was gathered. The remaining tissues were given 4 mL of fresh enzyme buffer and were digested for 15 min. The digestive process was repeated 7–9 times to ensure complete digestion. The supernatant collection from each round was centrifuged for 1 min at 1200 rpm, to obtain pellets of digested cells. The pellet was resuspended in DMEM/F12 culture medium (Gibco, USA) and plated onto 6 cm culture plates. 2 h after the initial plating, mCFs were obtained. MCFs were cultured in complete DMEM/F12 (10% FBS) at 37°C in 5% CO₂ and 95% air.

The si-CFRL, miR-3113-5p/-3473days mimic/inhibitor and corresponding negative controls (designed and synthesized by RiboBio, Guangzhou, China) were transfected into cells at 70–80% confluence using riboFECT CP Transfection Kit (RiboBio, Guangzhou, China) by the final concentrations of 50 nM for miRNA mimics and 100 nM for miRNA inhibitor and si-lncRNA. The plasmid DNA of CFRL and its negative control were purchased from Hanyin Biotechnology (Shanghai, China) and transfected into cells using LipofectamineTM 3000 Reagent (Invitrogen, Carlsbad, CA, USA) according to the manufacturer's instructions. CFs was induced by administering angiotensin II (AngII, 100 nM, Sigma, USA) after starvation in serum-free medium for 24 h.

METHOD DETAILS

Histological analysis

Hearts of mice were excised, fixed in 4% paraformaldehyde embedded with paraffin and sectioned into 7 μm slices, and stained with hematoxylin-eosin (HE). To measure cardiac fibrosis, we stained the heart sections with Sirius Red.

RNA fluorescence *in situ* hybridization (FISH)

The probe for CFRL was designed by Guangzhou Ribo, whose sequence covers the specific junction region of CFRL. The mCFs were cultured on cell slides in cell cultures plate until the cell confluence reach 60–70%. Then they were fixed by 4% paraformaldehyde on slides and were added hybridization solution away from light. DAPI was used for staining for 10 min and then washed by PBS buffer for 3 times. After mounting, the signal of the probe was detected by BaseScope Detection Reagent Kit (ACD, USA) according to the manufacturer's instructions. The images were acquired on Leica SP5 Spectral scanning laser confocal microscope (Leica Microsystems, Wetzlar, Germany).

Dual luciferase assay

The recombinant luciferase reporter plasmids (provided by RiboBio, Guangzhou, China) were constructed, containing the potential or mutated miR-3113-5p/miR-3473d binding site sequences in the 3'-UTR of CTGF/FN1 and CFRL. MCFs were seeded and co-transfected with corresponding plasmids and miRNA mimics. The cells were collected by passive lysis buffer 48 h later and assayed for luciferase activity with Dual-Luciferase Assay kit (Promega, USA). Firefly luciferase activities were normalized to Renilla luciferase activities.

Wound-healing assay

The mCFs were pre-cultured in 6-well plates (Nest Biotechnology, Jiangsu, China) and were transfected as above for 24 h. The cell monolayers were wounded by scratching with plastic 10- μL micropipette tips, washed 2 times with PBS, and fresh medium was added to the plates. Images were captured at 0, 6, 12, 24 h. Wound area was calculated by tracing the cell-free area in images using ImageJ software. The migration rate was expressed as the percentage of area reduction of wound closure. Wound closure% = $[(A_{t=0h} - A_{t=\Delta h}) / A_{t=0h}] \times 100\%$, where $A_{t=0h}$ was the area of the wound measured immediately after scratching (time zero), and $A_{t=\Delta h}$ was the area of the wound measured h hours after the scratch was performed³⁴.

CCK-8 cell viability assay

Cells were seeded in 96-well culture plates with a final volume of 100 μL and pre-incubated at 37°C with 5%CO₂ for 24 h. Subsequently, the cells were treated with corresponding reagents and cultured for another 24 h. After transfection, the Cell Counting Kit-8 assay was performed. 10 μL (10% of the volume) CCK-8 solution (Vazyme) was added to each well and incubated for 2 h. Then the absorbance at 450 nm was detected with a microplate reader (Bio-Rad, CA, USA).

Quantitative reverse transcription-PCR (qRT-PCR)

Total RNA was extracted from the LV tissues of mice and cultured mouse cardiac fibroblasts by FastPure Cell/Tissue Total RNA Isolation Kit (Vazyme, Nanjing, China). The NanoDrop One UV-Visible spectrophotometer (Thermo scientific, USA) was used to determine the concentration and purity of the extracted RNAs. MicroRNAs were reverse transcribed by using Bulge-loop RT primer and quantified with miRNA qPCR primer sets (both from RiboBio, Guangzhou, China). RNAs were reverse transcribed to cDNA according to the manufacturer's instructions for HiScript III RT SuperMix for qPCR (Vazyme, Nanjing, China). Quantitative RT-qPCR analysis was conducted on a Real-Time PCR System (Applied Biosystems) using SYBR qPCR Master Mix (Vazyme), cDNA template and specific primers (provided by Sangon Biotech, Shanghai, China). After the reactions, the cycle threshold (Ct) was determined, and relative RNA level was calculated and normalized to GAPDH (lncRNA and mRNA) or U6 (miRNA) level for each sample by the $2^{-\Delta\Delta C_t}$ method.

Western Blot

Total protein from the LV tissues and cardiac fibroblasts was extracted by RIPA lysis buffer containing protease inhibitors (Beyotime, Shanghai, China). The protein concentration was determined using BCA Protein Assay Kit (Beyotime, Shanghai, China). Protein samples were resolved in SDS-PAGE and transferred onto nitrocellulose membranes using an iBlot 2 dry blotting system (Thermo Fisher Scientific, USA). Then the membrane was blocked in 5% nonfat milk for 2 h and then probed with primary antibodies against fibronectin 1 (FN1, 1:1000), connecting tissue growth factor (CTGF, 1:1000), collagen type I alpha 1 chain (COL1A1, 1:1000), alpha-smooth muscle actin (α -SMA, 1:1000), β -actin (1:1000) or β -tubulin (1:1000) overnight at 4°C. Then, the membranes were incubated with peroxidase-conjugated anti-rabbit secondary antibodies (1:8000). All the antibodies were provided by Cell Signaling Technology. The signals were visualized using a chemiluminescence kit (Thermo Fisher Scientific, USA). Finally, the immunoreactivity was detected with the Luminescent Image Analyzer (GE Healthcare, Uppsala, Sweden). β -actin and β -tubulin protein levels were used as loading controls.

QUANTIFICATION AND STATISTICAL ANALYSIS

In each experiment, all determinations were performed at least in triplicate. All data were analyzed using Graphpad Prism V9.0 and presented as mean \pm SD. The normality of the data was first assessed with Shapiro-Wilk test. Statistical differences between two groups were determined by an unpaired, 2-tailed Student's t-test, and differences among 3 more groups were analyzed with one-way ANOVA followed by the Bonferroni post hoc analysis. In the data were not normally distributed, the unpaired 2-tailed Mann-Whitney U test (2 groups) or Kruskal-Wallis test (3 or more groups), followed by Dunn post hoc test, was used. A value of $p < 0.05$ was significant. * $p < 0.05$, ** $p < 0.01$, *** $p < 0.001$ vs. control.